Laminin-332 Cleavage by Matriptase Alters Motility Parameters of Prostate Cancer Cells

Manisha Tripathi[1], **Alka A. Potdar**[2], **Hironobu Yamashita**[1], **Brandy Weidow**[1], **Peter T. Cummings**[2,3], **Daniel Kirchhofer**[4], and **Vito Quaranta**[1,*]

[1]Department of Cancer Biology, Vanderbilt University Medical Center, Nashville, Tennessee

[2]Department of Chemical and Biomolecular Engineering, Vanderbilt University, Nashville, Tennessee

[3]Center for Nanophase Materials Sciences, Oak Ridge National Laboratory, Oak Ridge, Tennessee

[4]Department of Protein Engineering, Genentech, Inc., South San Francisco, California

Abstract

BACKGROUND—Matriptase, a type II transmembrane serine protease, has been linked to initiation and promotion of epidermal carcinogenesis in a murine model, suggesting that deregulation of its role in epithelia contributes to transformation. In human prostate cancer, matriptase expression correlates with progression. It is therefore of interest to determine how matriptase may contribute to epithelial neoplastic progression. One approach for studying this is to identify potential matriptase substrates involved in epithelial integrity and/or transformation like the extracellular matrix macromolecule, laminin-332 (Ln-332), which is found in the basement membrane of many epithelia, including prostate. Proteolytic processing of Ln-332 regulates cell motility of both normal and transformed cells, which has implications in cancer progression.

METHODS—In vitro cleavage experiments were performed with purified Ln-332 protein and matriptase. Western blotting, enzyme inhibition assays, and mass spectrometry were used to confirm cleavage events. Matriptase overexpressing LNCaP prostate cancer cells were generated and included in Transwell migration assays and single cell motility assays, along with other prostate cells.

RESULTS—We report that matriptase proteolytically cleaves Ln-332 in the β3 chain. Substrate specificity was confirmed by blocking cleavage with the matriptase inhibitor, Kunitz domain-1. Transwell migration assays showed that DU145 cell motility was significantly enhanced when plated on matriptase-cleaved Ln-332. Similarly, Transwell migration of matriptase-overexpressing LNCaP cells was significantly increased on Ln-332 and, as determined by live single-cell microscopy, two motility parameters of this cell line, speed and directional persistence, were also higher.

CONCLUSIONS—Proteolytic processing of Ln-332 by matriptase enhances speed and directional persistence of prostate cancer cells.

---

*Correspondence to: Vito Quaranta, MD, Department of Cancer Biology, Vanderbilt University School of Medicine, 771 Preston Research Building, 2220 Pierce Avenue, Nashville, TN 37232-6840., vito.quaranta@vanderbilt.edu.

Keywords

laminin-332; matriptase; type II transmembrane serine protease; proteolysis; prostate cancer; cell migration

INTRODUCTION

The American Cancer Society estimated that there would be ~192,280 new prostate cancer cases in the USA in 2009 alone [1]. In general, prostate cancer morbidity and mortality is due to metastasis, or the spread of cancer cells from their primary site to other tissues or organs in the body [2–5]. In order for cells to metastasize, they must first degrade nearby tissue barrier, the basal lamina (BL), and then migrate to secondary sites via the bloodstream or lymphatic system [3,4]. Degradation of BL takes place by cleavage of its extracellular matrix (ECM) components, like collagens and laminins, by enzymes like matrix metal-loproteinases (MMPs) or type II transmembrane serine proteases (TTSPs) [5,6]. These protease–ECM interactions have also been shown to contribute to cell migration, a critical component of invasion and metastasis [7–9].

One essential component of BL is laminin-332 (Ln-332: previously known as Ln-5 [10]), which is known to play an important role in development, wound healing, and tumorigenesis [11]. Ln-332 is reportedly overexpressed in many tumor types, including: esophageal, cutaneous, oral, laryngeal, colon, tracheal, and cervical cancers [12,13]. Interestingly, Ln-332 expression is instead decreased or lost in prostate cancer [14–17]. As depicted in Figure 1A, Ln-332 is a large multi-domain glycoprotein consisting of $\alpha 3$, $\beta 3$, and $\gamma 2$ subunits. It has a cross-shaped structure, with its long arm consisting of domains I and II, which holds the intact molecule together [13]. At its C-terminus, the $\alpha 3$ chain has five large globular (LG) domains that interact with various cell surface receptors, including integrins $\alpha 3\beta 1$, $\alpha 6\beta 4$, and heparin proteoglycan syndecans, which leads to establishment of cell adhesion and migration phenotype [9,13,18,19]. Through its N-terminus, the $\beta 3$ chain of Ln-332 interacts with other ECM molecules like Ln-6, Ln-7, and collagen VII, affecting BL assembly and cell-survival signaling [9,13]. The $\gamma 2$ chain contains epidermal growth factor (EGF)-like domains III-V [13] and interacts with epidermal growth factor receptor (EGFR), which also stimulates cell migration [9,20,21]. Of note, several studies have shown that all three Ln-332 chains can be processed by different protease systems [9]. In addition, some reports have suggested that these proteolytic events regulate cell motility of both normal and transformed cells [13], which may have implications in cancer progression.

Previously, our group has shown that Ln-332 $\gamma 2$ chain is cleaved by MMP2 and MT1-MMP [22,23]; others have shown that this chain is also cleaved by MMPs 3, 8, 12, 13, 14, and 20 [24], cathepsin S [25], mTLD [26], BMP-1 [27], and neutrophil elastase [28]. Furthermore, most of these studies have shown that processing of Ln-332 y2 chain by these proteases regulates cell migration [22,24,28]. Studies have also shown that Ln-332 $\beta 3$ chain is processed by MT1-MMP, which enhances prostate cancer cell migration compared to activity on uncleaved Ln-332 [29]. Another study reported that Ln-332 $\beta 3$ chain is a ligand for MMP7, which enhances cell motility of a colon carcinoma cell line [30]. It has also been reported that Ln-332 $\beta 3$ chain is cleaved at its N-terminus by endogenous proteinase(s) in human keratinocytes and other cell lines [31]; however, the specific protease involved in this cleavage has not been pinpointed. Directly relevant to this study, we previously demonstrated that Ln-332 $\beta 3$ chain is also cleaved by hepsin, 1 of 20 known TTSPs, which results in increased migration of prostate cancer cells in vitro [32]. Taken together, these studies establish that proteolytic processing of Ln-332 occurs physiologically and can alter cellular functions such as adhesion and migration [33,34].

Building on these previous findings, in this study we hypothesized that another TTSP upregulated in prostate cancer, matriptase (also named MT-SP1, TADG-15, epithin, and ST-14), would also cleave Ln-332 and in turn might have similar biological significance. The importance of matriptase in physiology is underscored by the fact that matriptase-deficient mice die shortly after birth due to a severely impaired water barrier function in the epidermis of skin and oral epithelium [35]. Furthermore, matriptase has recently been recognized as a potential marker for prostate cancer progression [36], as many studies have shown that matriptase expression is significantly increased in prostate tumor samples compared to normal tissue, and correlates with disease progression [36–38]. In addition, Forbs et al. [39] reported that inhibition of matriptase in prostate cancer cells by siRNA reduces their invasive growth potential in vitro; this group also reported a similar effect using a synthetic matriptase inhibitor. Another recent study found that a small molecule inhibitor against matriptase reduced growth of tumors in prostate cancer xenograft models [40]; these authors of this report also showed that tumor growth inhibition was through the attenuation of cancer cell invasion, rather than cell proliferation. A similar study showed reduction of cell migration and invasion using both in vitro and xenograft models by inhibiting matriptase by siRNA [41]. Matriptase is inhibited by the Kunitz domain (KD) of hepatocyte growth factor (HGF) activator inhibitor-1 (HAI-1), which is a Kunitz-type transmembrane serine protease inhibitor [42]. Using this inhibitor, it has been shown that inhibition of HAI-1 expression in prostate cancer cells results in increased cell invasion and migration in vitro [43]. Most recently, the strong oncogenic potential of matriptase has been firmly established by a report that showed transgenic mice with matriptase overexpression in the skin exhibited malignant transformation and had potentiated chemical carcinogenesis [44].

One of the key regulatory mechanisms of physiological and pathological functions by matriptase is by proteolytically processing or cleaving its substrates [45–49]. A few studies have demonstrated that matriptase can cleave the pro form of HGF, macro-phage-stimulating protein 1 (MSP-1), urokinase-type plasminogen activator, prostasin zymogen, Trask (transmembrane and associated with src kinases), and protease-activated receptor-2 [46,50–55]. However, further identification of critical substrates for matriptase is an important step in targeting this protease therapeutically for the treatment of prostate cancer. In this report, we demonstrate for the first time that matriptase cleaves Ln-332, which affects prostate cancer cell migration parameters. This study provides new insight into possible mechanisms for matriptase and Ln-332 in cancer progression.

MATERIALS AND METHODS

Cell Culture

The human prostate cancer cell line DU145 (American Type Culture Collection, Manassas, VA) and the rat bladder squamous carcinoma cell line 804G [43] were maintained in Dulbecco's modified Eagle's medium (DMEM; Life Technologies, Inc., Rockville, MD) supplemented with 10% fetal bovine serum (FBS; Gemini, Irvine, CA) and 1% glutamine/ penicillin/ streptomycin (g/p/s) antibiotics (Life Technologies, Inc.) in a humidified atmosphere containing 5% CO_2 at 37°C.

LNCaP prostate cancer cells expressing low (LNCaP-wt) and high levels (LNCaP-mt) of matriptase were created by Dr. Daniel Kirchhofer as detailed below (Genentech, San Francisco, CA), and were cultured in RPMI 1640 medium supplemented with 10% FBS, 500 μg/ml Geneticin (Invitrogen, Carlsbad, CA), 0.5 μg/ml puromycin (Sigma, St. Louis, MO), and 1% g/p/s antibiotics and incubated with 5% CO_2 at 37°C.

Purification of Rat Ln-332

Ln-332 was purified from spent medium of 804G rat bladder squamous carcinoma cells as previously described [32].

Cleavage of Ln-332 by Matriptase

To study the cleavage of Ln-332 by matriptase, purified rat Ln-332 (0.2 μM) was incubated with the human recombinant protease domain of matriptase (0.6, 2, and 6 μM). The reaction was performed in a buffer containing 250 mM NaCl and 50 mM Tris (pH 7.5) for 2–3 hr (as indicated) at 37°C. For the time course experiment, Ln-332 (0.8 μM) was incubated with matriptase (24 μM) and reaction buffer containing 250 mM NaCl and 50 mM Tris, pH 7.5, for 0, 3, 6, and 12 hr at 37°C. After incubation, sodium dodecyl sulfate–polyacrylamide gel electrophoresis (SDS–PAGE) was performed under reducing conditions on the matriptase and Ln-332 mixture (4–12% precasted gradient gels were used). Protein bands were visualized using SimplyBlue Safe Coomassie Blue stain (Invitrogen). Precision Plus™ protein dual color standard (BioRad, Hercules, CA) was used as a protein marker for comparison.

Western blot analysis was performed after transferring the reaction mixtures of Ln-332 with and without matriptase onto a PVDF membrane (Perkin Elmer, Waltham, MA) from the reducing gel. Polyclonal antibody (pAb) against the C-terminus of Ln-332 β3 chain (1:500; sc-20775; H-300; Santa Cruz Biotechnology, Inc., Santa Cruz, CA), and secondary anti-rabbit IgG HRP monoclonal antibody (1:5,000; GE Healthcare, UK) were used for Western blots. Protein bands were visualized with an ECL Plus system (Perkin Elmer). *ImageJ* was used for quantification of bands in the scanned Western blot film. Briefly, in the "Analyze" function of *ImageJ*, we "Set Measurements" for area, mean gray value, and integrated density. The bands of interest were selected and the parameters were measured. The raw intensity measurement for each band was normalized to its corresponding β-actin control.

Mass Spectrometry

The cleaved product of Ln-332 by matriptase was identified using mass spectrometry analysis performed by the Mass Spectrometry Research Center at Vander-bilt University (Nashville, TN). Briefly, after digestion, the proteins in the reaction mixture were separated by SDS–PAGE and visualized using Coomassie Blue stain. The protein bands of interest were excised from the SDS–PAGE gel. After further processing, trypsin digestion was performed and peptides were extracted and concentrated. For the preparation of sample for matrix-assisted laser desorption/ionization time-of-flight mass spectrometry (MALDI-TOF MS), 0.4 μl of the sample was applied to a target plate and overlaid with 0.4 μl alpha-cyano-4-hydroxycinnamic acid matrix (10 mg/ml in 60% acetonitrile, 0.1% trifluoroacetic acid). MALDI-TOF MS and tandem TOF/TOFMS/ MS were performed using a Voyager 4700 mass spectrometer (Applied Biosystems, Foster City, CA). TOF/TOF fragmentation spectra were acquired in a data-dependent fashion based on the MALDI-TOF peptide mass map for the protein. Both types of mass spectral data were collectively used to examine the protein databases to generate statistically significant candidate identification using GPS Explorer software (Applied Biosystems) running the MASCOT database search algorithm (Matrix Science, Inc., Boston, MA). Searches were performed against the SWISS PROT and the NCBI databases.

Matriptase Inhibition Assay

HAI-1-derived KD1 was used to inhibit enzymatic matriptase activity. KD1 is the N-terminal Kunitz domain of HAI-1 and was produced in *Escherichia coli* as described in Shia et al. [42]. As described in the Cleavage of Ln-332 by Matriptase Section above, purified rat

Ln-332 (0.2 μM) was incubated alone or with recombinant matriptase (6 μM) and reaction buffer with or without KD1 inhibitor (15 μM) for 2 hr at 37°C. SDS–PAGE was then performed and the gel was stained with Coomassie Blue.

Generation of Matriptase Overexpressing LNCaP Cells

The cDNA of full-length matriptase was inserted into a mammalian expression vector containing the puromycin resistance gene for antibiotic selection (Genentech). The LNCaP-luc clone [56] was transfected with the construct encoding full-length matriptase with a C-terminal FLAG tag, and the cells were selected with 0.5 μg/ml puromycin (Sigma–Aldrich). Clones were analyzed by FACS for matriptase surface expression using an anti-FLAG monoclonal antibody (Sigma– Aldrich). Two clones, one for the high matriptase expressor LNCaP-mt cells and one for the low matriptase expressor LNCaP-wt cells, were selected for further experiments.

LNCaP Cell Protein Isolation and Western Blot

LNCaP-wt and LNCaP-mt cells were lysed with RIPA buffer (25 mM Tris, pH 7.5, 150 mM NaCl, 1% Nonidet P-40, 1% sodium deoxycholate, and 0.1% SDS) containing protease inhibitor cocktail (Roche, Indianapolis, IN). Total protein levels of samples were measured using a bicinchoninic acid assay (Pierce, Thermo Fisher Scientific, Rockford, IL) and normalized. Denatured proteins were separated by SDS–PAGE and transferred for Western blotting. Non-specific binding to membranes was blocked for 1 hr with blocking buffer (5% milk in PBS). Blots were incubated overnight in primary antibody (1:1,000 pAb matriptase; Bethyl Laboratories, Inc., Montgomery, TX) or 1:1,000 monoclonal anti β-actin antibody (AC-74, Sigma) in blocking solution at 4°C, and subsequently in HRP conjugated anti-rabbit IgG and anti-mouse IgG secondary antibody (NA493v; GE Healthcare) for 1 hr at room temperature. Protein bands were visualized with an ECL Plus system (Amersham Pharmacia Biotech, Piscataway, NJ).

Transwell Cell Migration Assay

Modified Boyden chamber cell migration assays were performed using 8.0 μm pore size Transwell™ permeable supports (Corning Costar, Lowell, MA). The lower side of the filters were coated with either untreated or matriptase-treated rat Ln-332 with and without KD1, phosphate-buffered saline solution (PBS), or Ln-332 coincubated with matriptase and KD1 overnight at 4°C. Transwells were then blocked with 5% milk in PBS for 1 hr. Cells (DU145 or LNCaP) were trypsinized, resuspended in serum-free medium, and washed twice with serum-free medium. DU145 or LNCaP cells (20,000 or 50,000, respectively) were seeded in the upper chamber of inserts. After 5 hr (DU145) or 24 hr (LNCaP) incubation in cell culture conditions, cells remaining on the upper filter were scraped off using a cotton swab and the inserts were washed with PBS. Cells that migrated to the lower chamber were fixed with 400 µl of fixation solution (Hema-3® stain kit, cat. # 122–911, Fisher Scientific Company LLC, Kalamazoo, MI) for 10 min, and stained with 400 µl of staining solution for 20 min. Cells were manually counted using an inverted microscope equipped with a 10 × objective (Zeiss, Germany). Results are presented as the mean number of cells counted per field ±standard deviation. Student's t-tests were performed on final data to test significance of effects, with $P < 0.05$ accepted as significant.

Single Cell Motility Assay

LNCaP-wt or LNCaP-mt cells were plated (20,000 cells) overnight on 60-mm dishes coated with Ln-332 (10 μg/ml). Cell density was kept low to avoid interacting cell populations. Cells were monitored using phase-contrast optics in a Zeiss Axiovert 200 M inverted microscope with a monochrome, cooled CCD camera (CoolSNAP HQ, Roper Scientific,

Trenton, NJ) equipped with a temperature-controlled, humidified chamber. All cells were equilibrated in the humidified, temperature-controlled (37°C) microscope chamber for 30 min and media was replaced with fresh growth media prior to data collection. Images were both acquired and cells tracked using *Metamorph* (Molecular Devices Corporation, Sunnyvale, CA). Time-lapse images were collected at a magnification of $10 \times$ (1 pixel = 0.98 μm) using a sampling time interval of 1 min, for at least 12 hr in all experiments.

Cell Tracking

Each cell was tracked by following the cell nucleus using the "track objects" function in *Metamorph*. Only single cells were considered for the analysis; cells that remained stationary, moved outside the viewing area, underwent cell division, did not migrate over a distance of at least two cell bodies (<20 μm), or that adhered to other cells during the course of the experiment were excluded from the tracking procedure. Applying this criterion, ~60% cells were retained. Results are presented in combined box-and-whisker and scatter plots, which show the mean speed per population (dark horizontal line), 25th and 75th quartiles (box), 95% confidence intervals (whiskers), and raw data points (scatter). Mann–Whitney *U*-tests were performed on final data to test significance of effects, with $P < 0.05$ accepted as significant.

RESULTS

Ln-332 Is Cleaved by Matriptase

To determine whether matriptase cleaves Ln-332, purified Ln-332 from 804G rat bladder cells was incubated with three concentrations of the recombinant protease domain of matriptase for 2 hr. After incubation, the mixtures and Ln-332 alone were electro-phoresed on SDS–PAGE and then stained with Coomassie Blue. Ln-332 alone revealed four primary bands representing the α3 (190 kDa), β3 (145 kDa), and γ2 chains (155 and 80 kDa; Fig. 1B, lane 1) of the structure and matriptase alone revealed one strong band at ~27.5 kDa (lane 5). Of note, the lanes containing Ln-332 and matriptase mixtures revealed a unique band at ~100 kDa, particularly at higher concentrations of the latter (lanes 3 and 4, arrows). These lanes also resolved bands at ~27.5, ~18, and ~10 kDa, which were determined to be matriptase by mass spectrometry (data not shown). An additional SDS–PAGE gel that was instead run for 3 hr is shown in Supplemental Figure 1, which confirms the presence of a unique band at ~100 kDa after incubating Ln-332 with matriptase. These results suggest that the recombinant protease domain of matriptase cleaved Ln-332.

To determine if this cleavage was time-dependent, we also performed a time-course experiment whereby Ln-332 and matriptase were coincubated for 0, 3, 6, and 12 hr and the mixtures were again resolved using SDS–PAGE. As expected, no cleavage product of Ln-332 was observed in the 0 hr mixture, however, the cleaved ~100 kDa band was present in lanes containing the mixtures from 3, 6, and 12 hr (Fig. 1C, arrow).

Matriptase Cleaves the Ln-332 p3 Chain

To determine that the cleavage event of Ln-332 was due to addition of matriptase, and not another contamination protease, we also added a known inhibitor of matriptase, KD1, to the mixture. As in earlier experiments, purified rat Ln-332 alone revealed four bands, representing its respective chains (Fig. 2A, lane 1) and Ln-332 treated with matriptase again revealed the ~100 kDa cleavage product (lane 2). Of interest, the mixtures containing KD1 lacked the ~100 kDa cleavage product (lanes 3, 4; arrow), suggesting that matriptase was responsible for cleavage of Ln-332. Matriptase was again resolved as an ~27.5 kDa band, which matches up with the previous SDS–PAGE results, and KD1 was resolved as an ~11 kDa band, in line with our previous report [32].

To further determine the identity of the unique band that appeared after matriptase treatment of Ln-332, we used both Western blotting with an antibody to Ln-332 and a proteomics approach. As shown in Figure 2B, a pAb against the C-terminal sequence of Ln-332 β3 chain reacted with both the full-length β3 chain in Ln-332 alone and the ~100 kDa matriptase-cleaved fragment, as revealed by Western blotting. This result suggests that matriptase cleaves the β3 chain of Ln-332, possibly removing an N-terminal sequence. To explore this, we then performed mass spectrometric analysis. The protein bands of Ln-332 and the ~100 kDa product were excised from a gel from SDS–PAGE. After trypsin digestion, MALDI-TOF MS and tandem TOF/TOFMS/ MS were performed, and data from both methods were collectively used to examine the protein databases. Statistically significant candidates were identified using GPS Explorer software running the MASCOT database search algorithm. Searches were performed against the SWISS PROT and NCBI databases. The Ln-332 protein band contained its three chains: α3 (190 kDa), β3 (145 kDa), and γ2 (155 kDa). In addition, the digested ~100 kDa band that appeared upon treatment of Ln-332 with matriptase produced 19 different peptides that were identical to amino acid sequences of the Ln-332 β3 chain (Fig. 2C; peptides in gray).

Migration of DU145 Cells Is Enhanced on Ln-332 Cleaved by Matriptase

Since previous studies have shown that cleavage of the Ln-332 β3 chain by other proteases leads to changes in cell migration [9,32], we also investigated the effect of the cleavage of Ln-332 β3 chain by matriptase on prostate cancer cell migration in this study. First, we examined motility of DU145 cells using modified Boyden chambers treated with either untreated Ln-332, matriptase-cleaved Ln-332, PBS, or a mixture containing Ln-332, matriptase, and KD1. The number of cells that passed through filters after 5 hr were then manually counted under a microscope. As shown in Figure 3, cells seeded in chambers coated with matriptase-cleaved Ln-332 migrated significantly more (~1.6-fold) than cells on uncleaved Ln-332. In addition, cells in chambers treated with the Ln-332, matriptase, and KD1 inhibitor mixture migrated significantly less than cells on matriptase-cleaved Ln-332, which was similar to migration levels on untreated Ln-332.

Matriptase-Overexpression Enhances LNCaP Cell Migration on Ln-332

Since our experiments indicated that DU145 cell migration was increased on matriptase-cleaved Ln-332, we decided to also examine migration of LNCaP prostate cancer cells that stably overexpress matriptase (LNCaP-mt). Migration of these overexpressor cells was compared to that of wild-type LNCaP cells (LnCaP-wt) first using modified Boyden chamber assays. Prior to performing assays, we verified LNCaP cell expression by RT-PCR (data not shown) and Western blot (Fig. 4A); these results indicated that LNCaP-mt cells expressed ~2 times more matriptase than LNCaP-wt cells. For Boyden chamber assays, inserts were pretreated with either Ln-332 or PBS, and cells were allowed to migrate for 24 hr prior to counting the number of cells that passed through filters. As expected, LNCaP-mt cells exhibited significantly more migration than LNCaP-wt cells on Ln-332 (~3-fold; Fig. 4B,C). In contrast, both cell types migrated minimally on PBS-treated Transwells.

Matriptase-Overexpression Enhances Cell Speed and Directional Persistence

In order to acquire more detailed information about the motility of LNCaP cells, we also performed single-cell motility assays using high content microscopy. This technique involves tracking individual cell movement over time using video microscopy. In contrast to static Boyden chamber assays, this approach allows inspection of dynamic cell movement in real-time. Further, single-cell level parameters can help to model and predict population level behavior.

Time-lapse movies of LNCaP motility can be found in Supplementary Materials. In line with previous Boyden chamber results, the LNCaP-mt population moved significantly faster than LNCaP-wt cells using this technique (Fig. 5A). In addition, LNCaP-mt cells also moved in a more directed manner than LNCaP-wt cells, leading to significantly increased directionality ratios for this cell type (Fig. 5B). This ratio represents the *linear* distance a cell travels during an assay (d) versus the *total* distance traveled by that cell (t), which essentially captures cell persistence, or the tendency of a cell to continue moving in a particular direction without turning [57].

We also created Windrose plots by overlaying single cell tracks onto a single origin (0,0), in order to qualitatively assess the persistence for each cell type (Fig. 5C). Twelve-hour trajectories of LNCaP-wt (gray) and LNCaP-mt (black) cells are shown, which indicate that matriptase overexpressing cells are generally more persistent and travel farther than wt cells. The concentric circles superimposed on the plots indicate the root mean squared displacement (MSD) for each cell population after 12 hr. This value was obtained by first calculating the MSD for each cell population, using Equation (1), where $\vec{r}(t)$ is the position vector of the cell after time t, $\vec{r}(0)$ is the position at the beginning, and $\langle\ \rangle$ denotes the average over the entire cell population, followed by taking the square root of the MSD.

$$\text{MSD}=\left\langle\left(\vec{r}(t)-\vec{r}(0)\right)^2\right\rangle \quad \text{RMSD}=\sqrt{\text{MSD}} \quad (1)$$

In summary, these results show that the LNCaP-mt cell population covered a greater area than the LNCaP-wt population. Taken together, all single-cell motility parameters indicate that matriptase overexpressing cells exhibit a different migration phenotype than wild-type cells.

DISCUSSION

In this report, we studied two important steps of the metastatic cascade: breach of BL and cell migration [58]. Specifically, we have focused on investigating the interactions and effects of two potentially important players in prostate cancer progression: Ln-332, an essential BL component, and matriptase, 1 of 20 members of an emerging TTSP family [59,60]. The role of Ln-332 in prostate cancer has been of special interest because, in contrast to other tumors where Ln-332 is overexpressed, Ln-332 is instead reduced or lost in this type of cancer [14–16]. In contrast, matriptase is reportedly overexpressed in many cancers, including prostate, and its expression has been shown to correlate with disease progression [45,47–49]. Intuitively, this inversed expression of Ln-332 and matriptase in prostrate cancer suggests a potential interaction between these molecules during disease progression.

It has previously been shown that overexpression of matriptase in mouse epidermis induces spontaneous skin lesions in the absence of genetic alteration and independent of carcinogen exposure [44]. Furthermore, the authors showed that epidermal hyperproliferation and matriptase-induced tumors were abolished by coexpression of HAI-1. However, it remains to be determined how matriptase leads to neoplastic progression in such mouse models [44]. Matriptase is reportedly overexpressed in a wide variety of epithelial tumors, including breast, cervix, esophagus, liver, mesothelium, prostate, and colorectal cancers [36,38,61–69]. Interestingly, in the case of prostate cancer there is also correlation between matriptase expression and tumor grade [36–38]. The mechanism of action of matriptase remains to be determined, however, the possibilities include activation of growth factors, receptors, proteases, and the processing of ECM components. Identification of new substrates of

matriptase and definition of their biological function(s) upon cleavage contribute in unraveling the mechanistic action of matriptase in cancer.

Our results show, for the first time, that Ln-332 is proteolytically processed by matriptase in vitro. Mass spectrometry and Western blotting analyses indicated that catalytically active recombinant matriptase cleaves the β3 chain of Ln-332 and produces a novel ~100 kDa fragment (Fig. 1 and Fig. 2). Our previous work has shown that Ln-332 is also a substrate of another TTSP, hepsin [32]. Interestingly, both matriptase and hepsin cleave at the N-terminal of the Ln-332 β3 chain [32]. Proteolysis has been shown to be an important step in both physiological and pathological conditions [6,70]. One of the most widely reported effects of cleavage of Ln-332 has been increased cell migration [9,13]. It has been reported that MMPs generate a domain, DIII, from Ln-332 and binding of this domain to EGFR stimulates mitogen-activated protein kinase signaling, MMP-2 gene expression, and cell migration [20]. Also, it has been shown that processing of γ2 chain may influence Ln-332 turnover in BL and affect epithelial morphogenesis [23]. Although there are other protease systems that cleave Ln-332, we propose that the effects of cell surface proteases, including the family of TTSPs, have more physiological consequences than other protease systems due to their physiological positioning on the cell surface [55]. This locale gives such cell surface proteases access to ECM components, giving them an added advantage over other protease systems. In future studies, it would be worth screening whether all identified TTSPs possess the ability to cleave Ln-332, particularly at the β3 chain. In addition, it would be interesting to determine whether the cleavage site is conserved across species.

Our previous studies revealed that hepsin cleavage of Ln-332 increased cell migration [32], therefore we also investigated this function in this report. Modified Boyden chamber assays revealed that the human prostate cancer cell line, DU145, migrated significantly more on Ln-332 cleaved by matriptase than on intact Ln-332 substrate (Fig. 3). In line with this result, LNCaP prostate cancer cells overexpressing matriptase also migrated significantly more on Ln-332 than wild-type cells with a lower level of matriptase in Boyden chambers (Fig. 4). LNCaP cell motility was also analyzed at the single-cell level using high content microscopy for more in-depth study of cell dynamics. Interestingly, we found that single cells from both cell types exhibited variable speeds significantly different than the average for each population (Fig. 5), highlighting the importance of single-cell techniques for examining in-depth behavior. Furthermore, this analysis revealed that matriptase overexpressing cells migrated faster and more persistently than their corresponding control cells.

Cell migration studies are largely conducted at the population level (e.g., Boyden chamber), whereby a cell population is represented by an average measurement and some range of error. It is thought that in vivo single cell migration is required for metastasis through blood, whereas cohesive migration is required for lymphatic metastasis [71]. In this study, we investigated cell motility both at the population level and at the single-cell level using time-lapse video microscopy for slightly different purposes. Boyden chamber assays captured an end-point population level behavior of cells seeded at a high density. In contrast, single cell assays were performed at a lower cell density, and data were collected dynamically and assessed at both the single-cell and population levels. Recently, it was reported that two different phenotypic outcomes for cell migration may occur in vitro, dependent upon whether an investigator uses single-cell or cohesive migration strategies [72]. In other words, studying migration using these two different approaches investigates two different questions. In our case, change(s) in the migratory phenotype due to cleavage of Ln-332 by matriptase produced a similar result using both approaches. Intuitively, the increased number of LNCaP-mt cells that crossed through Boyden chambers can be explained by the single cell results, which show that matriptase overexpressing cells have increased speed and

persistence on Ln-332. Persistence in cell motion can be defined as the property by which a cell continues to migrate in one direction without much deviation (before changing its path) [57]. Studies have shown that cancer cell migration is directionally persistent, as in the cases of highly invasive cancers like neuroepithelial tumors [73] or epithelial cell over-expressing HER2 [74]. In addition, genetic modifications of biological molecules in a cell line have previously been shown to change the intrinsic pattern of cell migration [57]. However, to our knowledge, our report is the first study to show that overexpression of a cell surface protease leads to increased cell speed and persistence of cells plated on its substrates. Further analysis of single-cell assays must be performed to better understand whether the parameters obtained at this level can help in predicting their population level behavior.

Due to the limited availability of human Ln-332, most of the studies in this field (including ours) have been carried out using rat Ln-332. However, due to the functional interchangeability of ECM components across mammalian species, we are confident that one would see similar processing of human Ln-332 by matriptase. Interestingly, both hepsin and matriptase cleave the N-terminal of the Ln-332 β3 chain. Therefore, it is possible that cleavage of Ln-332 by these two TTSPs affects the interaction of Ln-332 with collagen VII, which in turn may effect hemidesmosome formation and tumor invasion, which has been previously reported [75]. Future studies should also be carried out to investigate this possibility.

We realize that the enzyme/substrate ratio used in this study is quite high. However, our rationale for choosing these ratios are based on the fact that Ln-332 is a bulky molecule with a molecular weight of 490 kDa, whereas the enzyme used in this study, the protease domain of matriptase, is only 27.5 kDa. For these reasons, many other previous studies using MMPs have also been performed at higher ratios in vitro [19,21,25,27]. As mentioned above, under physiological conditions, the TTSPs, including matriptase, are in close vicinity of the BM, thus they are also close to the substrate Ln-332.

CONCLUSIONS

In summary, we show that matriptase cleaves Ln-332 and this cleavage event results in increased migration of prostate cancer cells. LNCaP cells over-expressing matriptase migrated faster and in a more directionally persistent manner on Ln-332. Based on our findings, we propose that proteolytic processing of Ln-332 could be a possible mechanistic role for matriptase in prostate cancer progression via altered migration parameters and subsequent BL transgression. Therefore, identification of Ln-332 as one of the substrates for matriptase takes us one step closer to unraveling the mechanism(s) of action of matriptase.

Supplementary Material

Refer to Web version on PubMed Central for supplementary material.

Acknowledgments

REFERENCES

1. Jemal A, Siegel R, Ward E, Hao Y, Xu J, Thun MJ. Cancer statistics, 2009. CA Cancer J Clin. 2009; 59(4):225–249. [PubMed: 19474385]

2. Mundy GR. Metastasis to bone: Causes, consequences and therapeutic opportunities. Nat Rev Cancer. 2002; 2(8):584–593. [PubMed: 12154351]

3. Sherwood DR. Cell invasion through basement membranes: An anchor of understanding. Trends Cell Biol. 2006; 16(5):250–256. [PubMed: 16580836]

4. Chambers AF, Groom AC, MacDonald IC. Dissemination and growth of cancer cells in metastatic sites. Nat Rev Cancer. 2002; 2(8):563–572. [PubMed: 12154349]

5. Kalluri R. Basement membranes: Structure, assembly and role in tumour angiogenesis. Nat Rev Cancer. 2003; 3(6):422–433. [PubMed: 12778132]

6. Lopez-Otin C, Matrisian LM. Emerging roles of proteases in tumour suppression. Nat Rev Cancer. 2007; 7(10):800–808. [PubMed: 17851543]

7. Woodward JK, Holen I, Coleman RE, Buttle DJ. The roles of proteolytic enzymes in the development of tumour-induced bone disease in breast and prostate cancer. Bone. 2007; 41(6):912–927. [PubMed: 17945547]

8. Noel A, Gilles C, Bajou K, Devy L, Kebers F, Lewalle JM, Maquoi E, Munaut C, Remacle A, Foidart JM. Emerging roles for proteinases in cancer. Invasion Metastasis. 1997; 17(5):221–239. [PubMed: 9876217]

9. Hintermann E, Quaranta V. Epithelial cell motility on laminin-5: Regulation by matrix assembly, proteolysis, integrins and erbB receptors. Matrix Biol. 2004; 23(2):75–85. [PubMed: 15246107]

10. Aumailley M, Bruckner-Tuderman L, Carter WG, Deutzmann R, Edgar D, Ekblom P, Engel J, Engvall E, Hohenester E, Jones JC, Kleinman HK, Marinkovich MP, Martin GR, Mayer U, Meneguzzi G, Miner JH, Miyazaki K, Patarroyo M, Paulsson M, Quaranta V, Sanes JR, Sasaki T, Sekiguchi K, Sorokin LM, Talts JF, Tryggvason K, Uitto J, Virtanen I, von der Mark K, Wewer UM, Yamada Y, Yurchenco PD. A simplified laminin nomenclature. Matrix Biol. 2005; 24(5): 326–332. [PubMed: 15979864]

11. Ryan MC, Christiano AM, Engvall E, Wewer UM, Miner JH, Sanes JR, Burgeson RE. The functions of laminins: Lessons from in vivo studies. Matrix Biol. 1996; 15(6):369–381. [PubMed: 9049976]

12. Guess CM, Quaranta V. Defining the role of laminin-332 in carcinoma. Matrix Biol. 2009; 28(8): 445–455. [PubMed: 19686849]

13. Marinkovich MP. Tumour microenvironment: Laminin 332 in squamous-cell carcinoma. Nat Rev Cancer. 2007; 7(5):370–380. [PubMed: 17457303]

14. Hao J, Jackson L, Calaluce R, McDaniel K, Dalkin BL, Nagle RB. Investigation into the mechanism of the loss of laminin 5 (alpha3beta3gamma2) expression in prostate cancer. Am J Pathol. 2001; 158(3):1129–1135. [PubMed: 11238061]

15. Nagle RB. Role of the extracellular matrix in prostate carcinogenesis. J Cell Biochem. 2004; 91(1): 36–40. [PubMed: 14689579]

16. Calaluce R, Beck SK, Bair EL, Pandey R, Greer KA, Hoying AM, Hoying JB, Mount DW, Nagle RB. Human laminin-5 and laminin-10 mediated gene expression of prostate carcinoma cells. Prostate. 2006; 66(13):1381–1390. [PubMed: 16804886]

17. Davis TL, Cress AE, Dalkin BL, Nagle RB. Unique expression pattern of the alpha6beta4 integrin and laminin-5 in human prostate carcinoma. Prostate. 2001; 46(3):240–248. [PubMed: 11170153]

18. Yamashita H, Shang M, Tripathi M, Jourquin J, Georgescu W, Liu S, Weidow B, Quaranta V. Epitope mapping of function-blocking monoclonal antibody CM6 suggests a "weak" integrin binding site on the laminin-332 LG2 domain. J Cell Physiol. 2010; 223(3):541–548. [PubMed: 20301201]

19. Yamashita H, Tripathi M, Harris MP, Liu S, Weidow B, Zent R, Quaranta V. The role of a recombinant fragment of laminin-332 in integrin alpha3beta1-dependent cell binding, spreading and migration. Biomaterials. 2010; 31(19):5110–5121. [PubMed: 20347131]

20. Schenk S, Hintermann E, Bilban M, Koshikawa N, Hojilla C, Khokha R, Quaranta V. Binding to EGF receptor of a laminin-5 EGF-like fragment liberated during MMP-dependent mammary gland involution. J Cell Biol. 2003; 161(1):197–209. [PubMed: 12695504]

21. Schenk S, Quaranta V. Tales from the crypt[ic] sites of the extracellular matrix. Trends Cell Biol. 2003; 13(7):366–375. [PubMed: 12837607]

22. Giannelli G, Falk-Marzillier J, Schiraldi O, Stetler-Stevenson WG, Quaranta V. Induction of cell migration by matrix metal-loprotease-2 cleavage of laminin-5. Science. 1997; 277(5323):225–228. [PubMed: 9211848]

23. Koshikawa N, Schenk S, Moeckel G, Sharabi A, Miyazaki K, Gardner H, Zent R, Quaranta V. Proteolytic processing of laminin-5 by MT1-MMP in tissues and its effects on epithelial cell morphology. FASEB J. 2004; 18(2):364–366. [PubMed: 14688206]

24. Pirila E, Sharabi A, Salo T, Quaranta V, Tu H, Heljasvaara R, Koshikawa N, Sorsa T, Maisi P. Matrix metalloproteinases process the laminin-5 gamma 2-chain and regulate epithelial cell migration. Biochem Biophys Res Commun. 2003; 303(4):1012–1017. [PubMed: 12684035]

25. Wang B, Sun J, Kitamoto S, Yang M, Grubb A, Chapman HA, Kalluri R, Shi GP. Cathepsin S controls angiogenesis and tumor growth via matrix-derived angiogenic factors. J Biol Chem. 2006; 281(9):6020–6029. [PubMed: 16365041]

26. Veitch DP, Nokelainen P, McGowan KA, Nguyen TT, Nguyen NE, Stephenson R, Pappano WN, Keene DR, Spong SM, Greenspan DS, Findell PR, Marinkovich MP. Mammalian tolloid metalloproteinase, and not matrix metalloprotease 2 or membrane type 1 metalloprotease, processes laminin-5 in keratino-cytes and skin. J Biol Chem. 2003; 278(18):15661–15668. [PubMed: 12473650]

27. Amano S, Scott IC, Takahara K, Koch M, Champliaud MF, Gerecke DR, Keene DR, Hudson DL, Nishiyama T, Lee S, Greenspan DS, Burgeson RE. Bone morphogenetic protein 1 is an extracellular processing enzyme of the laminin 5 gamma 2 chain. J Biol Chem. 2000; 275(30): 22728–22735. [PubMed: 10806203]

28. Mydel P, Shipley JM, Adair-Kirk TL, Kelley DG, Broekelmann TJ, Mecham RP, Senior RM. Neutrophil elastase cleaves laminin-332 (laminin-5) generating peptides that are chemotactic for neutrophils. J Biol Chem. 2008; 283(15):9513–9522. [PubMed: 18178964]

29. Udayakumar TS, Chen ML, Bair EL, Von Bredow DC, Cress AE, Nagle RB, Bowden GT. Membrane type-1-matrix metalloproteinase expressed by prostate carcinoma cells cleaves human laminin-5 beta3 chain and induces cell migration. Cancer Res. 2003; 63(9):2292–2299. [PubMed: 12727852]

30. Remy L, Trespeuch C, Bachy S, Scoazec JY, Rousselle P. Matrilysin 1 influences colon carcinoma cell migration by cleavage of the laminin-5 beta3 chain. Cancer Res. 2006; 66(23):11228–11237. [PubMed: 17145868]

31. Nakashima Y, Kariya Y, Yasuda C, Miyazaki K. Regulation of cell adhesion and type VII collagen binding by the beta3 chain short arm of laminin-5: Effect of its proteolytic cleavage. J Biochem. 2005; 138(5):539–552. [PubMed: 16272566]

32. Tripathi M, Nandana S, Yamashita H, Ganesan R, Kirchhofer D, Quaranta V. Laminin-332 is a substrate for hepsin, a protease associated with prostate cancer progression. J Biol Chem. 2008; 283(45):30576–30584. [PubMed: 18784072]

33. Carter WG, Kaur P, Gil SG, Gahr PJ, Wayner EA. Distinct functions for integrins alpha 3 beta 1 in focal adhesions and alpha 6 beta 4/bullous pemphigoid antigen in a new stable anchoring contact (SAC) of keratinocytes: Relation to hemidesmosomes. J Cell Biol. 1990; 111(6 Pt 2):3141–3154. [PubMed: 2269668]

34. Belkin AM, Stepp MA. Integrins as receptors for laminins. Microsc Res Tech. 2000; 51(3):280–301. [PubMed: 11054877]

35. List K, Haudenschild CC, Szabo R, Chen W, Wahl SM, Swaim W, Engelholm LH, Behrendt N, Bugge TH. Matriptase/MT-SP1 is required for postnatal survival, epidermal barrier function, hair follicle development, and thymic homeostasis. Oncogene. 2002; 21(23):3765–3779. [PubMed: 12032844]

36. Saleem M, Adhami VM, Zhong W, Longley BJ, Lin CY, Dickson RB, Reagan-Shaw S, Jarrard DF, Mukhtar H. A novel biomarker for staging human prostate adenocarcinoma: Overexpression

of matriptase with concomitant loss of its inhibitor, hepatocyte growth factor activator inhibitor-1. Cancer Epidemiol Bio-markers Prev. 2006; 15(2):217–227.

37. Warren M, Twohig M, Pier T, Eickhoff J, Lin CY, Jarrard D, Huang W. Protein expression of matriptase and its cognate inhibitor HAI-1 in human prostate cancer: A tissue microarray and automated quantitative analysis. Appl Immunohistochem Mol Morphol. 2009; 17(1):23–30. [PubMed: 18813126]

38. Riddick AC, Shukla CJ, Pennington CJ, Bass R, Nuttall RK, Hogan A, Sethia KK, Ellis V, Collins AT, Maitland NJ, Ball RY, Edwards DR. Identification of degradome components associated with prostate cancer progression by expression analysis of human prostatic tissues. Br J Cancer. 2005; 92(12):2171–2180. [PubMed: 15928670]

39. Forbs D, Thiel S, Stella MC, Sturzebecher A, Schweinitz A, Steinmetzer T, Sturzebecher J, Uhland K. In vitro inhibition of matriptase prevents invasive growth of cell lines of prostate and colon carcinoma. Int J Oncol. 2005; 27(4):1061–1070. [PubMed: 16142324]

40. Galkin AV, Mullen L, Fox WD, Brown J, Duncan D, Moreno O, Madison EL, Agus DB. CVS-3983, a selective matriptase inhibitor, suppresses the growth of androgen independent prostate tumor xenografts. Prostate. 2004; 61(3):228–235. [PubMed: 15368474]

41. Sanders AJ, Parr C, Davies G, Martin TA, Lane J, Mason MD, Jiang WG. Genetic reduction of matriptase-1 expression is associated with a reduction in the aggressive phenotype of prostate cancer cells in vitro and in vivo. J Exp Ther Oncol. 2006; 6(1):39–48. [PubMed: 17228523]

42. Shia S, Stamos J, Kirchhofer D, Fan B, Wu J, Corpuz RT, Santell L, Lazarus RA, Eigenbrot C. Conformational lability in serine protease active sites: Structures of hepatocyte growth factor activator (HGFA) alone and with the inhibitory domain from HGFA inhibitor-1B. J Mol Biol. 2005; 346(5):1335–1349. [PubMed: 15713485]

43. Sanders AJ, Parr C, Mason MD, Jiang WG. Suppression of hepatocyte growth factor activator inhibitor-1 leads to a more aggressive phenotype of prostate cancer cells in vitro. Int J Mol Med. 2007; 20(4):613–619. [PubMed: 17786295]

44. List K, Szabo R, Molinolo A, Sriuranpong V, Redeye V, Murdock T, Burke B, Nielsen BS, Gutkind JS, Bugge TH. Deregulated matriptase causes ras-independent multistage carcinogenesis and promotes ras-mediated malignant transformation. Genes Dev. 2005; 19(16):1934–1950. [PubMed: 16103220]

45. Bugge TH, List K, Szabo R. Matriptase-dependent cell surface proteolysis in epithelial development and pathogenesis. Front Biosci. 2007; 12:5060–5070. [PubMed: 17569630]

46. Darragh MR, Bhatt AS, Craik CS. MT-SP1 proteolysis and regulation of cell-microenvironment interactions. Front Biosci. 2008; 13:528–539. [PubMed: 17981566]

47. List K. Matriptase: A culprit in cancer? Future Oncol. 2009; 5(1):97–104. [PubMed: 19243302]

48. List K, Bugge TH, Szabo R. Matriptase: Potent proteolysis on the cell surface. Mol Med. 2006; 12(1–3):1–7. [PubMed: 16838070]

49. Uhland K. Matriptase and its putative role in cancer. Cell Mol Life Sci. 2006; 63(24):2968–2978. [PubMed: 17131055]

50. Bhatt AS, Erdjument-Bromage H, Tempst P, Craik CS, Moasser MM. Adhesion signaling by a novel mitotic substrate of src kinases. Oncogene. 2005; 24(34):5333–5343. [PubMed: 16007225]

51. Netzel-Arnett S, Currie BM, Szabo R, Lin CY, Chen LM, Chai KX, Antalis TM, Bugge TH, List K. Evidence for a matriptase-prostasin proteolytic cascade regulating terminal epidermal differentiation. J Biol Chem. 2006; 281(44):32941–32945. [PubMed: 16980306]

52. Bhatt AS, Welm A, Farady CJ, Vasquez M, Wilson K, Craik CS. Coordinate expression and functional profiling identify an extracellular proteolytic signaling pathway. Proc Natl Acad Sci USA. 2007; 104(14):5771–5776. [PubMed: 17389401]

53. Lee SL, Dickson RB, Lin CY. Activation of hepatocyte growth factor and urokinase/plasminogen activator by matriptase, an epithelial membrane serine protease. J Biol Chem. 2000; 275(47): 36720–36725. [PubMed: 10962009]

54. Seitz I, Hess S, Schulz H, Eckl R, Busch G, Montens HP, Brandl R, Seidl S, Schomig A, Ott I. Membrane-type serine protease-1/matriptase induces interleukin-6 and −8 in endothelial cells by activation of protease-activated receptor-2: Potential implications in atherosclerosis. Arterioscler Thromb Vasc Biol. 2007; 27(4):769–775. [PubMed: 17255532]

55. Takeuchi T, Harris JL, Huang W, Yan KW, Coughlin SR, Craik CS. Cellular localization of membrane-type serine protease 1 and identification of protease-activated receptor-2 and single-chain urokinase-type plasminogen activator as substrates. J Biol Chem. 2000; 275(34):26333–26342. [PubMed: 10831593]

56. Moran P, Li W, Fan B, Vij R, Eigenbrot C, Kirchhofer D. Pro-urokinase-type plasminogen activator is a substrate for hepsin. J Biol Chem. 2006; 281(41):30439–30446. [PubMed: 16908524]

57. Pankov R, Endo Y, Even-Ram S, Araki M, Clark K, Cukierman E, Matsumoto K, Yamada KM. A Rac switch regulates random versus directionally persistent cell migration. J Cell Biol. 2005; 170(5):793–802. [PubMed: 16129786]

58. Hanahan D, Weinberg RA. The hallmarks of cancer. Cell. 2000; 100(1):57–70. [PubMed: 10647931]

59. Bugge TH, Antalis TM, Wu Q. Type II transmembrane serine proteases. J Biol Chem. 2009; 284(35):23177–23181. [PubMed: 19487698]

60. Szabo R, Bugge TH. Type II transmembrane serine proteases in development and disease. Int J Biochem Cell Biol. 2008; 40(6–7):1297–1316. [PubMed: 18191610]

61. Cheng MF, Tzao C, Tsai WC, Lee WH, Chen A, Chiang H, Sheu LF, Jin JS. Expression of EMMPRIN and matriptase in esophageal squamous cell carcinoma: Correlation with clinico-pathological parameters. Dis Esophagus. 2006; 19(6):482–486. [PubMed: 17069593]

62. Hoang CD, D'Cunha J, Kratzke MG, Casmey CE, Frizelle SP, Maddaus MA, Kratzke RA. Gene expression profiling identifies matriptase overexpression in malignant mesothelioma. Chest. 2004; 125(5):1843–1852. [PubMed: 15136399]

63. Tsai WC, Chao YC, Lee WH, Chen A, Sheu LF, Jin JS. Increasing EMMPRIN and matriptase expression in hepatocellular carcinoma: Tissue microarray analysis of immunohistochemical scores with clinicopathological parameters. Histopathology. 2006; 49(4):388–395. [PubMed: 16978202]

64. Tsai WC, Chu CH, Yu CP, Sheu LF, Chen A, Chiang H, Jin JS. Matriptase and survivin expression associated with tumor progression and malignant potential in breast cancer of Chinese women: Tissue microarray analysis of immunostaining scores with clinicopathological parameters. Dis Markers. 2008; 24(2):89–99. [PubMed: 18219094]

65. Lee JW, Yong Song S, Choi JJ, Lee SJ, Kim BG, Park CS, Lee JH, Lin CY, Dickson RB, Bae DS. Increased expression of matriptase is associated with histopathologic grades of cervical neoplasia. Hum Pathol. 2005; 36(6):626–633. [PubMed: 16021568]

66. Tanimoto H, Shigemasa K, Tian X, Gu L, Beard JB, Sawasaki T, O'Brien TJ. Transmembrane serine protease TADG-15 (ST14/ Matriptase/MT-SP1): Expression and prognostic value in ovarian cancer. Br J Cancer. 2005; 92(2):278–283. [PubMed: 15611789]

67. Santin AD, Cane S, Bellone S, Bignotti E, Palmieri M, De Las Casas LE, Anfossi S, Roman JJ, O'Brien T, Pecorelli S. The novel serine protease tumor-associated differentially expressed gene-15 (matriptase/MT-SP1) is highly overexpressed in cervical carcinoma. Cancer. 2003; 98(9):1898–1904. [PubMed: 14584072]

68. Kang JY, Dolled-Filhart M, Ocal IT, Singh B, Lin CY, Dickson RB, Rimm DL, Camp RL. Tissue microarray analysis of hepatocyte growth factor/Met pathway components reveals a role for Met, matriptase, and hepatocyte growth factor activator inhibitor 1 in the progression of node-negative breast cancer. Cancer Res. 2003; 63(5):1101–1105. [PubMed: 12615728]

69. Oberst MD, Johnson MD, Dickson RB, Lin CY, Singh B, Stewart M, Williams A, al-Nafussi A, Smyth JF, Gabra H, Sellar GC. Expression of the serine protease matriptase and its inhibitor HAI-1 in epithelial ovarian cancer: Correlation with clinical outcome and tumor clinicopathological parameters. Clin Cancer Res. 2002; 8(4):1101–1107. [PubMed: 11948120]

70. Rowe RG, Weiss SJ. Breaching the basement membrane: Who, when and how? Trends Cell Biol. 2008; 18(11):560–574. [PubMed: 18848450]

71. Ozerlat I. Cell migration: The benefit of being single. Nat Rev Mol Cell Biol. 2009; 10(12):816. [PubMed: 19950447]

72. Giampieri S, Manning C, Hooper S, Jones L, Hill CS, Sahai E. Localized and reversible TGFbeta signalling switches breast cancer cells from cohesive to single cell motility. Nat Cell Biol. 2009; 11(11):1287–1296. [PubMed: 19838175]

73. Deisboeck TS, Demuth T, Mansury Y. Correlating velocity patterns with spatial dynamics in glioma cell migration. Acta Biotheor. 2005; 53(3):181–190. [PubMed: 16329007]

74. Kumar N, Zaman MH, Kim HD, Lauffenburger DA. A high-throughput migration assay reveals HER2-mediated cell migration arising from increased directional persistence. Biophys J. 2006; 91(4):L32–L34. [PubMed: 16782798]

75. Ortiz-Urda S, Garcia J, Green CL, Chen L, Lin Q, Veitch DP, Sakai LY, Lee H, Marinkovich MP, Khavari PA. Type VII collagen is required for Ras-driven human epidermal tumorigenesis. Science. 2005; 307(5716):1773–1776. [PubMed: 15774758]
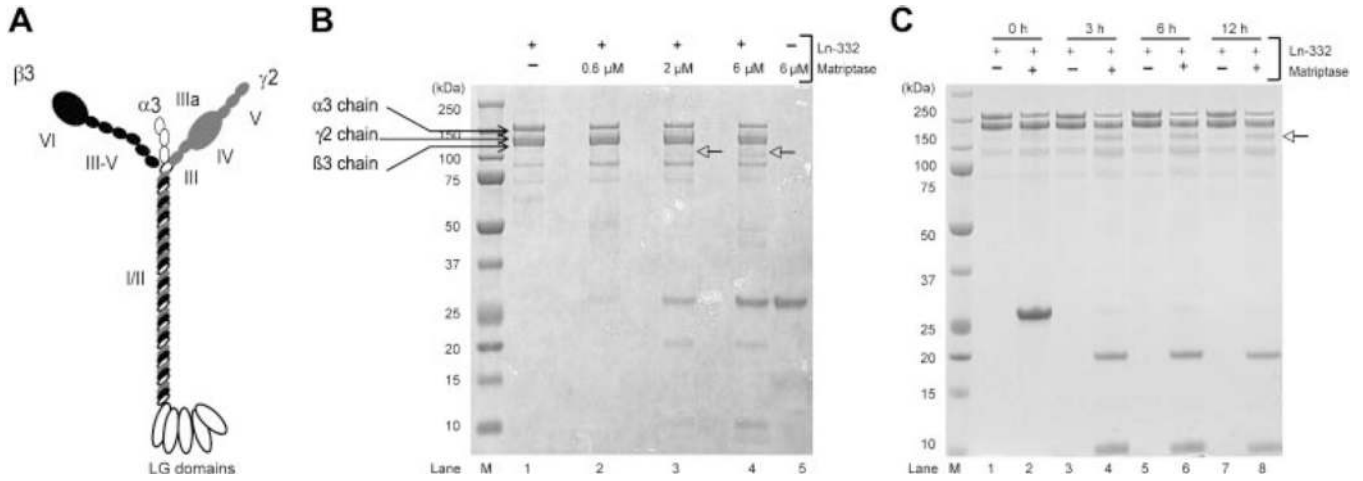
Fig. 1.
Ln-332 is cleaved by matriptase. **A**: Schematic of Ln-332 structure, which is composed of α3, β3, and γ2 chains. **B**: Purified Ln-332 from 804G rat bladder cells (0.2 μM) was incubated with the recombinant protease domain of matriptase (0.6,2, and 6 μM) for 2 hr. After incubation, the mixtures and Ln-332 alone were electrophoresed on SDS–PAGE and then stained with Coomassie blue. Ln-332 alone revealed four primary bands representing the α3 (190 kDa), β3 (145 kDa), and γ2 chains (155 and 80 kDa; lane I). Of note, a unique band was resolved at ~I00 kDa in the lanes containing Ln-332 and matriptase, particularly at higher concentrations of the latter (lanes 3 and 4, arrows). **C**: Ln-332 (0.8 μM) and matriptase (24 μM) were coincubated for 0, 3,6, and 12 hr. No cleavage product of Ln-332 was observed from the 0 hr mixture, however, the cleaved ~I00 kDa band was present in lanes containing the mixtures from 3,6, and 12 hr (arrow).
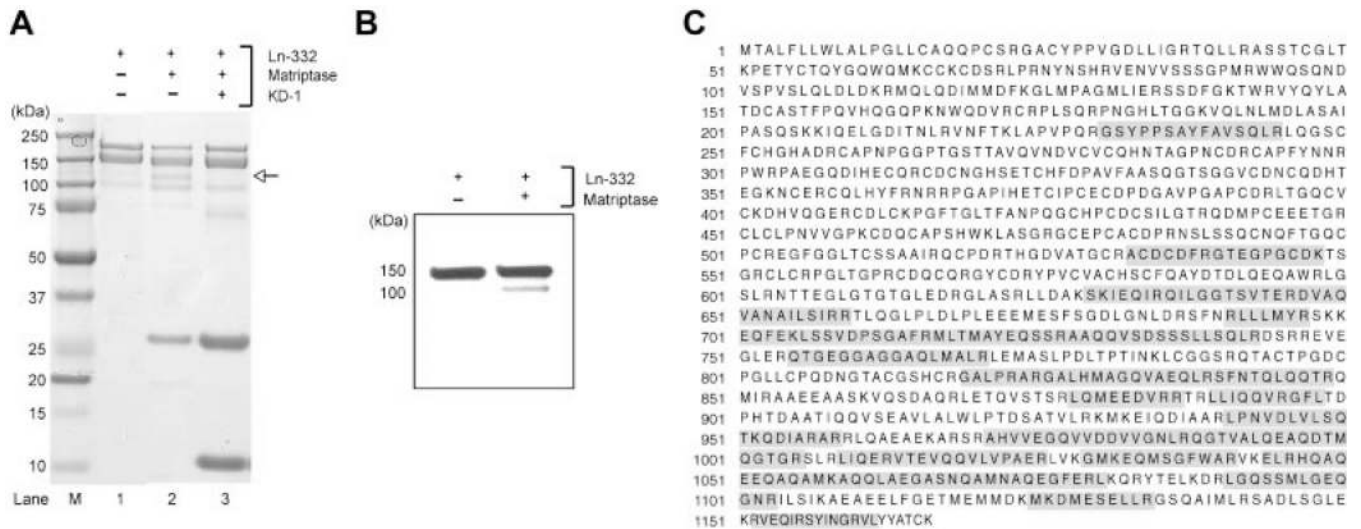
A

Ln-332 / Matriptase / KD-1 (lane labels)

(kDa): 250, 150, 100, 75, 50, 37, 25, 20, 15, 10

Lane M 1 2 3

B

Ln-332 / Matriptase

(kDa): 150, 100

C

```
   1  MTALFLLWLALPGLLCAQQPCSRGACYPPVGDLLIGRTQLLRASSTCGLT
  51  KPETYCTQYGQWQMKCCKCDSRLPRNYNSHRVENVVSSSGPMRWWQSQND
 101  VSPVSLQLDLDKRMQLQDIMMDFKGLMPAGMLIERSSDFGKTWRVYQYLA
 151  TDCASTFPQVHQGQPKNWQDVRCRPLSQRPNGHLTGGKVQLNLMDLASAI
 201  PASQSKKIQELGDITNLRVNFTKLAPVPQRGSYPPSAYFAVSQLRLQGSC
 251  FCHGHADRCAPNPGGPTGSTTAVQVNDVCVCQHNTAGPNCDRCAPFYNNR
 301  PWRPAEGQDIHECQRCDCNGHSETCHFDPAVFAASQGTSGGVCDNCQDHT
 351  EGKNCERCQLHYFRNRRPGAPIHETCIPCECDPDGAVPGAPCDRLTGQCV
 401  CKDHVQGERCDLCKPGFTGLTFANPQGCHPCDCSILGTRQDMPCEEETGR
 451  CLCLPNVVGPKCDQCAPSHWKLASGRGCEPCACDPRNSLSSQCNQFTGQC
 501  PCREGFGGLTCSSAAIRQCPDRTHGDVATGCRACDCDFRGTEGPGCDKTS
 551  GRCLCRPGLTGPRCDQCQRGYCDRYPVCVACHSCFQAYDTDLQEQAWRLG
 601  SLRNTTEGLGTGTGLEDRGLASRLLDAKSKIEQIRQILGGTSVTERDVAQ
 651  VANAILSIRRTLQGLPLDLPLEEEMESFSGDLGNLDRSFNRLLLMYRSKK
 701  EQFEKLSSVDPSGAFRMLTMAYEQSSRAAQQVSDSSSLLSQLRDSRREVE
 751  GLERQTGEGGAGGAQLMALRLEMASLPDLTPTINKLCGGSRQTACTPGDC
 801  PGLLCPQDNGTACGSHCRGALPRARGALHMAGQVAEQLRSFNTQLQQTRQ
 851  MIRAAEEAASKVQSDAQRLETQVSTSRLQMEEDVRRTRLLIQQVRGFLTD
 901  PHTDAATIQQVSEAVLALWLPTDSATVLRKMKEIQDIAARLPNVDLVLSQ
 951  TKQDIARARRLQAEAEKARSRAHVVEGQVVDDVVGNLRQGTVALQEAQDTM
1001  QGTGRSLRLIQERVTEVQQVLVPAERLVKGMKEQMSGFWARVKELRHQAQ
1051  EEQAQAMKAQQLAEGASNQAMNAQEGFERLKQRYTELKDRLGQSSMLGEQ
1101  GNRILSIKAEAEELFGETMEMMDKMKDMESELLRGSQAIMLRSADLSGLE
1151  KRVEQIRSYINGRVLYYATCK
```

Fig. 2.
Matriptase cleaves the Ln-332 β3 chain. **A**: A known matriptase inhibitor, KDI, was added to the Ln-332 and matriptase mixture. Purified rat Ln-332 (0.2 μM) alone revealed four bands, representing its respective chains (lane I). Ln-332 (0.2 μM) treated with matriptase (6 μM) again revealed the ~100 kDa cleavage product (lane 2). The mixture also containing KDI lacked the ~100 kDa cleavage product (lanes 3 and 4). **B**: A Western blot was performed using a pAb against the C-terminal sequence of Ln-332 β3 chain.The antibody reacted with both the full-length β3 chain in Ln-332 alone and the ~100 kDa matriptase-cleaved fragment.**C**: Mass spectrometry was performed to analyze the contents of the protein bands of Ln-332 and the ~100 kDa product from Ln-332 treated with matriptase. This analysis revealed that the Ln-332 protein band contained its three chains: α3 (190 kDa), β3 (145 kDa), and γ2 (155 kDa), and the digested ~I00 kDa band that appeared upon treatment of Ln-332 with matriptase produced 19 different peptides (gray) that were clearly identical to amino acid sequences of Ln-332 β3 chain.
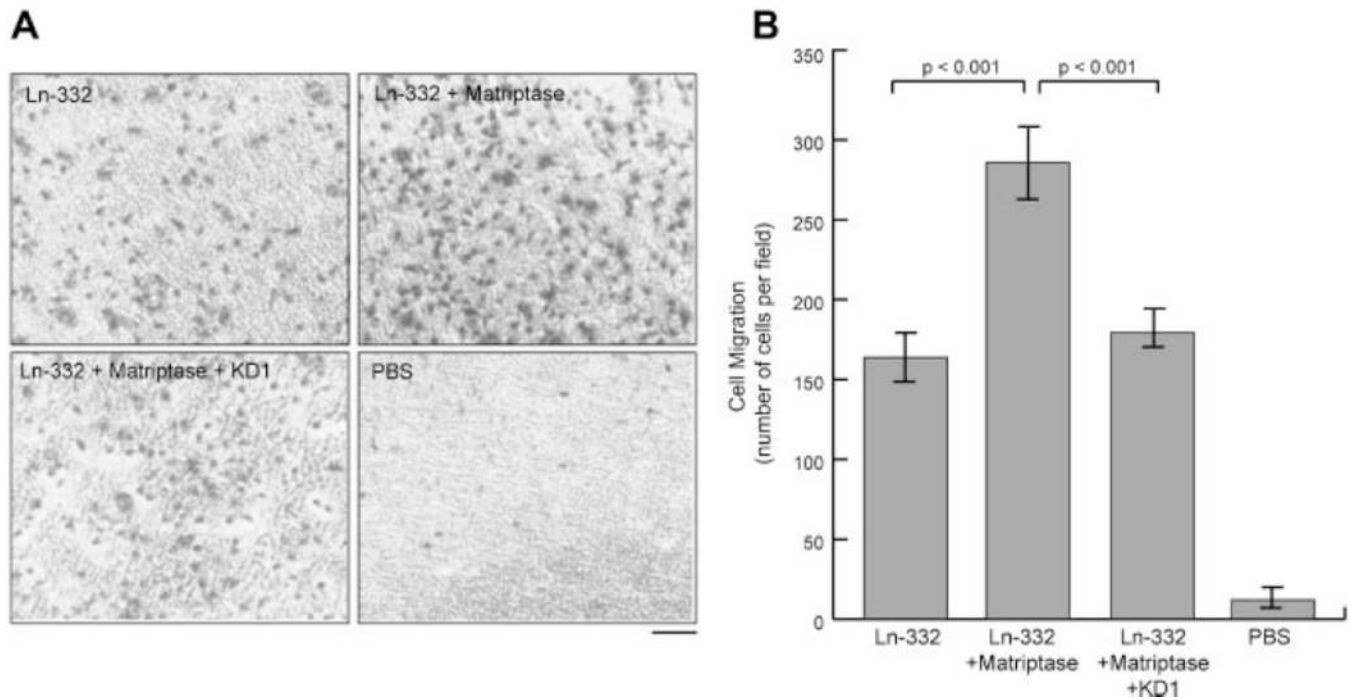
Fig. 3.
Migration of DU145 cells is enhanced on Ln-332 cleaved by matriptase. **A**: DU145 prostate cancer cell migration was measured using Boyden chambers coated with either untreated Ln-332 or matriptase-cleaved Ln-332. Some filters were also coated with either PBS or a mixture containing Ln-332, matriptase, and KD1.The number of cells that passed through filters after 5 hr were then manually counted under a microscope. **B**: Cells seeded in chambers coated with matriptase-cleaved Ln-332 exhibited significantly more migration (~1.6-fold) than cells on uncleaved Ln-332 (N = 2, in duplicate; $P < 0.001$). Further, cells in chambers coated with the Ln-332, matriptase, and KDI inhibitor mixture exhibited significantly less migration than those cells on matriptase-cleaved Ln-332 (N = 2, in duplicate; $P < 0.001$), similar to levels on untreated Ln-332.
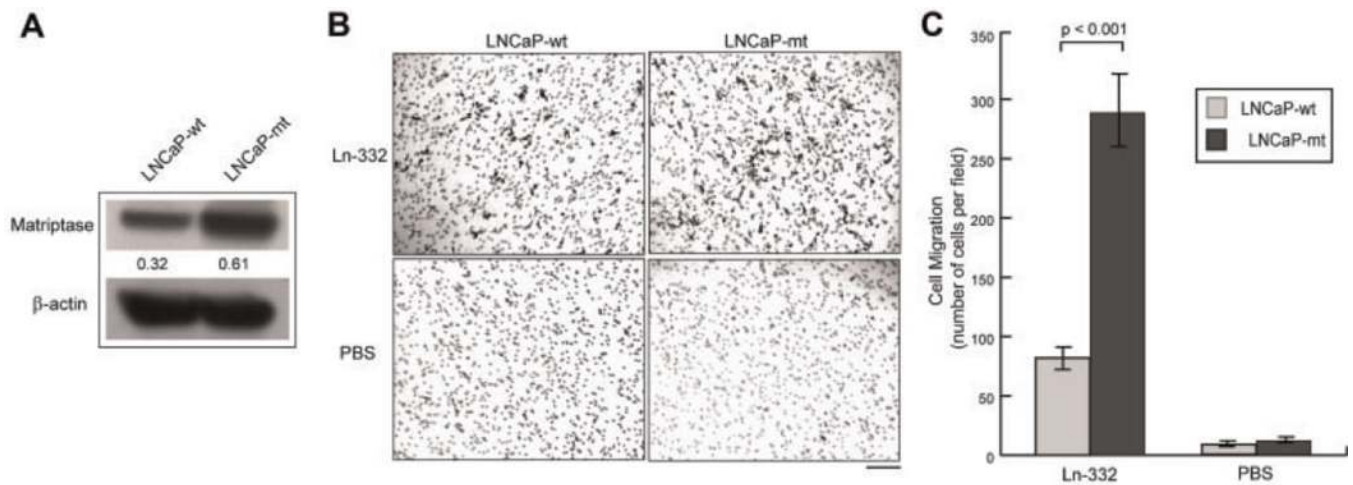
Fig. 4.
Matriptase-overexpression enhances LNCaP cell migration on Ln-332. **A**: Matriptase expression of both types of LNCaP cells was confirmed by Western blot. Band intensity for each sample was normalized to its corresponding β-actin control. These results indicated that LNCaP-mt cells express ~2 times more matriptase than LNCaP-wt cells. **B**: Boyden chamber assay was used to examine cell migration of both LNCaP-wt and LNCaP-mt cell types.Transwells were coated with either Ln-332 (10 μg/ml) or PBS, cells were allowed to migrate for 24 hr, and cells that migrated across the filter were fixed, stained, and counted manually under a microscope. **C**: LNCaP-mt cells exhibited significantly more migration than LNCaP-wt cells on Ln-332 (~3-fold; N = 3, in duplicate; $P < 0.001$). In contrast, both cell types migrated minimally on PBS-treated inserts.
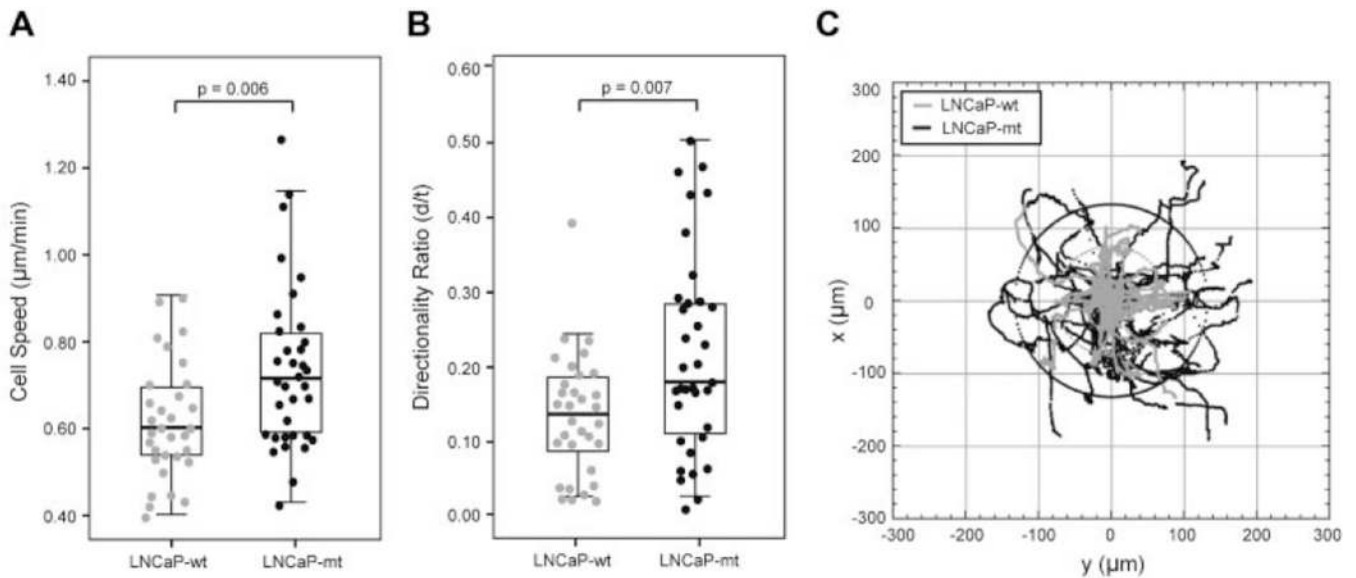
Fig. 5.

Matriptase-overexpression enhances cell speed and directional persistence. **A**: Single-cell motility assays were performed using high content microscopy. Individual cell speed was measured using Metamorph software.The LNCaP-mt cell population moved significantly faster than LNCaP-wt cells using this technique (N = 32 and 35 cells, respectively; P = 0.006). Box and whisker plots show the population mean (bold horizontal line), 25th and 75th quartiles (box), and 95% confidence intervals (whiskers) overlaid on raw single-cell data (scatter). **B**: LNCaP-mt cells were also found to move in a more directed manner than LNCaP-wt cells, leading to significantly increased directionality ratios for this cell type, which represents the *linear* distance a cell travels during an assay (d) versus the *total* distance traveled by that celI (t).**C**:Windrose plots were made to qualitatively examine the persistence for these cell types; these plots overlay all cell tracks (from *x* and *y* coordinates) starting with a common origin (0,0). Twelve-hour trajectories of LNCaP-*wt* (gray) and LNCaP-*mt* (black) cells are shown, which indicate that, in general, the matriptase overexpressing cells are more persistent and travel further than wt cells. The circles superimposed on the Windrose plots indicate the root mean squared dispersal for each cell type.